Aggregation behavior of fullerenes in aqueous solutions: a capillary electrophoresis and asymmetric flow-field flow fractionation study

Alina Astefanei[a], Oscar Núñez[a,b,*], Maria Teresa Galceran[a], Wim Th. Kok[c], Peter J. Schoenmakers[c]

[a]Department of Analytical Chemistry, University of Barcelona.Martí i Franquès 1-11, E08028 Barcelona, Spain.

[b] Serra Húnter Fellow, Generalitat de Catalunya, Spain.

[c]Analytical Chemistry Group-HIMS, University of Amsterdam, PO Box 94157, 1090 GD, Amsterdam, The Netherlands

* Corresponding author: Oscar Núñez

Department of Analytical Chemistry, University of Barcelona
Martí i Franquès 1-11, E-08028, Barcelona, Spain.
Phone: 34-93-403-3706
Fax: 34-93-402-1233
e-mail: oscar.nunez@ub.edu

Abstract

In this work the electrophoretic behaviour of hydrophobic fullerenes (C_{60}, C_{70} and C_{60}-pyrr) and water soluble fullerenes ($C_{60}(OH)_{24}$, $C_{120}(OH)_{30}$, C_{60}-pyrr tris acid and $C_{60}CHCOOH$) in micellar electrokinetic capillary chromatography (MECC) was evaluated. The aggregation behavior of the water soluble compounds in MECC at different buffer and SDS concentrations and pH values of the background electrolyte (BGE) was studied by monitoring the changes observed in the electrophoretic pattern of the peaks. Broad and distorted peaks that can be attributed to fullerene aggregation were obtained in MECC which became narrower and more symmetric by working at low buffer and SDS concentrations (below the critical micelle concentration, capillary zone electrophoresis (CZE) conditions). For the characterization of the suspected aggregates formed (size and shape), asymmetrical flow field-flow fractionation (AF4) and transmission electron microscopy (TEM) were used. The results showed that the increase in the buffer concentration promoted the aggregation of the particles while the presence of SDS micelles revealed multiple peaks corresponding to particles of different aggregation degree. Furthermore, MECC has been applied for the first time for the analysis of C_{60} in two different cosmetic products (*i.e.*, anti-aging serum and facial mask).

KEYWORDS: Capillary Zone Electrophoresis; Cosmetic products; Micellar Electrokinetic Capillary Chromatography; Asymmetric flow-field flow fracitonation; Fullerene aggregates

Abbreviations: Fullerol ($C_{60}(OH)_{24}$), Polyhydroxy small gap fullerene, hydrated ($C_{120}(OH)_{30}$), N-methyl-fulleropyrrolidine (C_{60}-pyrr), C_{60} pyrrolidine tris acid (C_{60}-pyrr tris acid), (1,2-Methanofullerene C60)-61-carboxylic acid ($C_{60}CHCOOH$)

1. Introduction

Since the discovery of buckminsterfullerene (C_{60}) [1] fullerene nanoparticles have been widely investigated for their exploitation within biological systems [2], cosmetic products [3], electronics and photovoltaics [4]. The unique physicochemical properties of pristine and especially of surface modified fullerenes make them promising therapeutic and diagnostic agents showing surprising properties and biocompatibility [5-7]. In particular, fullerols which are surface modified C_{60} -fullerenes with (poly)hydroxy functional groups can be ideal candidates for the treatment of neuro-degenerative disorders (*e.g.* Parkinson's and Alzheimer's disease) [6]. Carboxy-fullerene derivatives have potential use in photodynamic therapy [8] and as inhibitors of the HIV-1 protease [9]. However, it was reported that fullerenes are retained in the body for long periods [10] raising concerns about their potential chronic toxic effects. At nanoscale level, even subtle changes in their physicochemical properties can significantly alter their biocompatibility and application [11].

Pristine and surface modified fullerene aggregate in aqueous media leading to the formation of structures of various shapes and sizes depending on the type and number of the functional groups attached to the carbon cage [12-15]. These physicochemical properties impact their mobility, fate, bioavailability and toxicity [16,17]. Nevertheless, there is a significant lack of knowledge on fullerene exposure, and there are conflicting reports on their potential risks. To determine their behavior and distribution, analytical methods adequate for their separation and quantitation have to be developed. Liquid chromatography coupled to mass spectrometry (LC-MS) is the most frequently method used for the analysis of fullerenes in complex matrices but most of the reported studies are focused on hydrophobic compounds [15,18] and only few have been dedicated to the analysis of water soluble fullerenes such as fullerols [19,20].

Capillary electrophoretic (CE) techniques have also been used to analyze fullerenes. For the separation of hydrophobic fullerenes, nonaqueous capillary electrophoresis (NACE) [21-23] by employing charged salts and organic solvent mixtures as separation medium has been reported. The behavior of C_{60} and of a C_{60}-C_{70} mixture in micellar electrokinetic capillary chromatography (MECC) has also been evaluated [24]. This last work also studied the use of C_{60} and C_{70} encapsulated in sodium docecylsulfate (SDS) micelles (i.e. SDS[C_{60}] and SDS[C_{70}] complexes) as pseudostationary phase for the separation of polyaromatic hydrocarbons (PAHs) by

MECC. Regarding water soluble fullerene derivatives, both capillary zone electrophoresis (CZE) and MECC with SDS micelles were reported [25-27]. Among these studies, only two addressed the analysis of some carboxy-fullerene derivatives [25,27] and to the best of our knowledge there are no reports about the analysis of fullerols. In this context, Chan *et al.* [27] evaluated the use of CZE and MECC for the analysis of two water soluble fullerene derivatives (carboxy-fullerene (C3) and dendro[60]fullerene (DF)) in human serum samples and recommended using CZE for the quantitation of both compounds, presenting some advantages over MECC such as lower analysis time, better reproducibility and lower detection limits. Moreover, the presence of SDS micelles increased the number of electrophoretic peaks of DF complicating its analysis in the real samples. The behavior of DF in CZE as a function of pH, ionic strength, solvent amount and concentration of additives has been also reported [26]. The parameters which showed the most important effect on the migration time and electrophoretic peak profile were the pH and the ionic strength. The migration time of DF increased with the pH and decreased with the salt concentration in reversed polarity. The application of CE techniques for the determination of fullerenes in complex samples is very limited. Fullerenes are increasingly used in commercial applications, such as cosmetic/pharmaceutical products, at relatively high concentration levels (i.e., mg L^{-1} levels) making these kind of samples suitable to be quantified by CE techniques [15]. However, to the best of our knowledge there is only one study reporting the analysis of C_{60} in a cosmetic product by a CE technique (i.e., NACE) [21].

Although CE is mainly a separation technique, it has also been applied for the study of the aggregation behavior of low and high molecular weight species by monitoring changes in the electrophoretic pattern of the peaks (presence of multiple and/or broad peaks) [28-30] although there are no studies involving fullerene compounds.

Asymmetrical flow field-flow fractionation (AF4) is an open channel separation technique able to characterize (macro) molecules and particles in solution and to calculate the hydrodynamic radius (r_H) of the particles from the retention time [31,32]. Although this technique is increasingly used for nanoparticles characterization [33], the number of studies devoted to fullerenes characterization is limited and most of the reports are focused on hydrophobic compounds [15,34-36]. Concerning water soluble fullerenes, there is only one study [37] that used AF4 combined with atomic force

microscopy (AFM) to evaluate the aggregate sizes and morphology of fullerol reporting r_H of ≈ 2 nm in Milli-Q water which increased at higher ionic strength.

The aim of this work is to study the aggregation behavior of several surface modified fullerenes, two polyhydrody-fullerenes ($C_{60}(OH)_{24}$, $C_{120}(OH)_{30}$) and two carboxy-fullerene derivatives (C_{60}CHCOOH and C_{60}-pyrr tris acid) not previously reported, at varying buffer and SDS concentrations by CE and to characterize the aggregates by asymmetrical flow-field flow fractionation (AF4). For this purpose, the effect of the BGE composition (*i.e.*, buffer and SDS concentration and pH) on the electrophoretic migration time and peak profile was evaluated and AF4 was used to determine the aggregate sizes of the selected fullerenes in the tested CE conditions. In addition, TEM was employed to visualize the morphology of the selected compounds in the conditions employed for the electrophoretic studies. In addition, MECC was used for the first time for the determination of C_{60} in two cosmetic products.

2. Materials and methods

2.1. Chemicals and standard solutions

C_{60}, C_{70}, C_{60}-pyrr, $C_{120}(OH)_{30}$, C_{60}CHCOOH and C_{60}-pyrr tris acid were purchased from Sigma-Aldrich (Steinheim, Germany). $C_{60}(OH)_{24}$ was supplied by Materials & Electrochemical Research M.E.R. Corporation (Tucson, Arizona, USA). The chemical structures and abbreviations of these compounds are given in Figure 1.

Sodium phosphate, sodium chloride, sodium tetraborate, and SDS were purchased from Sigma-Aldrich (Steinheim, Germany). Sudan III, sodium hydroxide, hydrochloric acid were obtained from Merck (Darmstadt, Germany).

Water was purified using an Elix 3 coupled to a Milli-Q system (Millipore, Bedford, MA, USA) and filtered using a 0.22 µm nylon filter integrated into the Milli-Q system.

For the preparation of the SDS[C_{60}], SDS[C_{70}] and SDS[C_{60}-pyrr] complexes, individual stock solutions in toluene (~1000 mg Kg^{-1}) and SDS aqueous solutions (100 mM) were used. The stock solutions in 100 mM SDS (~ 30 mg L^{-1} SDS[C_{60}]and SDS[C_{60}-pyrr]and ~ 10 mg L^{-1} SDS[C_{70}]) were obtained by mixing the exact amounts of each solution in individual amber vials and treated in an ultrasonic bath until the toluene was completely evaporated and the aqueous phase became transparent brownish-yellow

(SDS[C_{60}], C_{60}-pyrr) and dark-purple (SDS[C_{70}]). The working solutions were diluted with the appropriate amount of SDS 100 mM prior to analysis.

Stock standard solutions of $C_{120}(OH)_{30}$ and $C_{60}(OH)_{24}$ (~1000 mg Kg^{-1}) were individually prepared by weight in Milli-Q water and stored at 4°C. The aqueous suspensions of the carboxy-fullerene derivatives were obtained first by dissolving the solid powder in tetrahydrofuran (Merck, Darmstadt, Germany), and the appropriate amount of Milli-Q water (depending on the final fullerene concentration) was added to the solution. Next, the solution was sonicated until the tetrahydrofuran was completely evaporated to obtain stock solutions of approximately 500 mg Kg^{-1}. Prior to analysis, each stock solution was diluted with the appropriate amount of Milli-Q water to obtain the working solution.

2.2. Instrumentation

2.2.1. Capillary electrophoresis(CE)

CE experiments were performed on a Beckman P/ACE MDQ capillary electrophoresis instrument (Fullerton, CA, USA) equipped with a diode array detector. CE separations were carried out using uncoated fused-silica capillaries (Beckman) with a total length of 50 cm (45 cm effective length) x 75 µm I.D. (375 µm O.D.). CZE and MECC analysis were performed by using 2 mM SDS in 1 mM sodium tetraborate and 100 mM SDS in 10 mM sodium phosphate-10 mM sodium tetraborate solutions, respectively, as BGEs. The capillary temperature was held at 25 ˚C. The BGE was filtered through a 0.45 µm nylon membrane filter before use. A capillary voltage of + 20 kV was applied for the separations. Sample introduction was performed by hydrodynamic injection (10 s, 13.5 kPa). Direct UV detection was performed at 254 nm. The CE instrument was controlled using Beckman 32 Karat software version 5.0.

New capillaries were pre-treated with 0.1 M HCl for 30 min, water for 30 min, 1 M NaOH for 30 min, and finally washed with water for 30 min. At the beginning of each session, the capillary was rinsed with 0.5 M NaOH for 10 min, with water for 10 min, and with the BGE for 15 min. The capillary was rinsed with the BGE for 5 min between runs and stored after rinsing with water at the end of each session.

2.2.2. Asymmetrical flow-field flow Fractionation (AF4)

The fractionation was carried out with an Eclipse Dualtec AF4 separation system (Wyatt Technology Europe GmbH, Dernbach, Germany) equipped with a programmable pump (Isocratic 1100, Agilent Technologies), an Agilent 1100 series degasser and an Agilent 1200 series auto sampler/injector. A mini-channel (11cm in length, 22 mm in width at the injection point and 3 mm close to the end) was equipped with a 480 µm spacer of trapezoidal shape and Millipore regenerated cellulose (RC) membrane of 10 kDa nominal molar mass cut-off (Superon GmbH, Dernbach, Germany). On-line detection was performed with a UV detector (Applied Biosystems, Foster City, California, USA).

The samples were injected in Milli-Q water with an injection flow of 0.1 mL min^{-1}. The relaxation and focusing were carried out during a specific time (3 min for the carboxy-fullerenes and 10 min for polyhydroxy-fullerene derivatives) at a cross flow rate of 2 mL min^{-1}. Time-delayed exponential (TDE) mode was used for the elution step with a delay/decay time of 3 min (carboxy-fullerenes) and 7 min (polyhydroxy-fullerene derivatives), an initial cross flow of 2 mL min^{-1} and a channel flow of 1 mL min^{-1}. The eluted samples were monitored by the UV detector at 254 nm.

2.2.3. Transmission electron microscopy (TEM)

For TEM measurements, one drop of the aqueous fullerene solutions prepared in 100 mM SDS and 10 mM sodium tetraborate-10 mM sodium phosphate was placed on a TEM grid (carbon-coated copper grid 200 mesh (All Carbon)) and stained with a drop of uranyl formate (1% aqueous solution). After air drying of the grid (2 h), TEM images were taken.

2.3. Sample preparation

The extraction of C_{60} from the cosmetic products (*i.e.*, anti- aging serum and a facial mask) was performed by following a procedure previously described [21] with few modifications. Briefly, for the extraction approx. 3 g of cosmetic sample were added to 20 mL toluene and sonicated for 4 h. The toluene extract was then centrifuged at 4500 rot/min for 15 min using a Selecta Centronic Centrifuge (Barcelona, Spain). The clear toluene supernatant was then evaporated to almost dryness, and reconstituted in 200 µL of 100 mM SDS aqueous solution, and the residual toluene was completely evaporatedvia sonication prior to be injected into the CE system.

3. Results

3.1. Hydrophobic fullerenes

In this work, the performance of MECC for the analysis of hydrophobic fullerenes (C_{60}, C_{70} and C_{60}-pyrr) using as BGE 100 mM SDS in 10 mM sodium phosphate-10mM sodium tetraborate (pH=9.4), previously proposed by Treubig and Brown [24] was evaluated. The compounds were first solubilized in aqueous media via interaction with SDS micelles following the procedure included in the *Materials and methods* Section. Figure 2A shows an example of the electropherogram obtained for the analysis of SDS[C_{60}] appearing as a sharp peak at the migration time of approx. 18 min. Electropherograms with the same migration time indicating identical electrophoretic mobility were also obtained for C_{70} and C_{60}-pyrr. The instrumental quality parameters such as limits of detection (LOD), limits of quantitation (LOQs) based on signal-to-noise ratio of 3:1 and 10:1 respectively, linearity and precision were evaluated for each compound using standard fullerene solutions prepared in SDS (100 mM) and are given in Table 1. The LODs ranged from 0.6 to 2.2 mg L^{-1}, and the calibration curves based on peak areas at concentration ranges between 0.8 and 30 mg L^{-1} (SDS[C_{60}] and SDS[C_{60}-pyrr]) and between 2.2 and 10 mg L^{-1} (SDS[C_{70}]) showed good linearity with correlation coefficients (r^2) of 0.991 (C_{60}), 0.994 (C_{60}-pyrr) and 0.988 (C_{70}). Run-to-run and day-to-day precisions were calculated at two concentration levels, at low level (LOQ) and a medium level (15 mg L^{-1} for SDS[C_{60}] and SDS[C_{60}-pyrr] and 5 mg L^{-1} for SDS[C_{70}]), and the results expressed as relative standard deviation (% RSD), are given in Table 1. As can be seen, acceptable run-to-run and day-to-day precisions were achieved with RSD values lower than 14.3 %.

This MECC method was used to determine C_{60} in two commercial cosmetic products (face mask and anti-aging serum) that contain this compound using 100 mM SDS in 10 mM sodium phosphate-10mM sodium tetraborate as running electrolyte. Sample extractions were performed as indicated in the *Sample preparation* section and the extracts were analyzed using the proposed MECC method. As an example, the obtained electropherogram for one of the analyzed samples and of the same product fortified with C_{60} is shown in Figure 2B. Since no blank samples were available, quantitation was carried out by triplicate using a standard addition method, and C_{60} was quantitated at 1.86 ± 0.07 mg L^{-1} (anti-aging serum) and 2.77 ± 0.16 mg kg^{-1} (face mask) concentration levels.

3.2. Polyhydroxy- and carboxy-fullerene derivatives

In a first step, polyhydroxy- and carboxy-fullerene derivatives were analyzed by MECC using the BGE employed for the analysis of hydrophobic fullerenes (100 mM SDS, 10 mM sodium phosphate-10mM sodium tetraborate, pH=9.4 solution). Figure 3 shows the electropherograms obtained for each of the studied compounds ($C_{60}(OH)_{24}$, $C_{120}(OH)_{30}$, C_{60}-pyrr tris acid and $C_{60}CHCOOH$). Under these conditions, broad and distorted peaks were obtained for all the fullerenes. $C_{60}(OH)_{24}$ and $C_{60}CHCOOH$ presented peak tailing and fronting, respectively and the electropherograms of $C_{120}(OH)_{30}$ and C_{60}-pyrr tris acid revealed broad and multiple peaks. Subsequently, the effect of the buffer and SDS concentration and pH value on the migration time and electrophoretic peak profile of the selected analytes was evaluated.

The effect of the buffer composition and concentration was studied by keeping constant the SDS concentration (100 mM) and pH value (≈ 9.4). Figure 4 shows the electropherograms obtained for the studied compounds at different buffer composition and concentrations. As can be seen, highly broad and distorted peaks were obtained for all the fullerenes at high buffer concentration values (above 10 mM sodium tetraborate-10 mM sodium phosphate) and for some of the compounds multiple peaks were observed. For instance, the electropherograms of C_{60}-pyrr tris acid revealed two unresolved peaks and the tail of the first one increased so much that at 15 mM sodium tetraborate-15mM sodium phosphate, it embraced migration times from 4 to 11 min. For all the compounds, the migration times decreased with a decrease in the buffer concentration and their electrophoretic pattern changed, revealing sharper peaks at 2.5 mM sodium tetraborate-2.5 mM sodium phosphate buffer concentration. A further improvement in peak shapes was obtained by using only sodium tetraborate as buffer at a concentration of 1 mM (Figure 4).

The changes in the electrophoretic profile of the peaks were further monitored at SDS concentration values between 2 and 100 mM (Figure 5) using 1 mM sodium tetraborate as buffer. In general, lower migration times and narrower peaks were obtained by reducing the SDS concentration in the running BGE and in some cases, changes in the peak profile were observed. For instance, the electropherogram of C_{60}-pyrr tris acid, at SDS concentrations ≥ 40 mM, showed two peaks and below this value only one peak was observed although its symmetry worsened showing front tailing. In contrast, for $C_{60}CHCOOH$ a more symmetrical peak is obtained at low SDS

concentration. Regarding the studied polyhydroxy-fullerene derivatives in addition to a reduction of the retention times, the number of distinguishable peaks decreased with the SDS concentration (see as an example the electropherograms obtained for $C_{120}(OH)_{30}$ in Fig. 5). Moreover, when working in CZE conditions, using SDS concentrations below the critical micellar concentration (CMC, 8 mM) and a low buffer concentration, narrower peaks than those found in MECC were obtained.

4. Discussion

4.1. Hydrophobic fullerenes

It has been reported that C_{60} forms aggregates within SDS micelles [24,38,39] but despite this fact, MECC has not been proposed for the analysis of this compound. Therefore, the capability of this electrophoretic method for the analysis of C_{60} but also of C_{70} and C_{60}-pyrr for which there is no information in the literature was evaluated in this work. The MECC electropherograms obtained for the resulting fullerene-SDS complexes analyzed individually indicated that interaction occurred and the three compounds were completely entrapped in the hydrophobic core of the micelles. The migration time of the three compounds was that of the micelles which was measured using Sudan III. Therefore, this technique can only be applied for the analysis of individual hydrophobic fullerenes in quality control analysis where only one of these compounds is present. The quality parameters were evaluated in order to use the method for the determination of the individual compounds in samples where the other fullerenes are not expected. The results showed good repeatability and reproducibility and the obtained LOQs (Table 1) allowed us to propose the MECC method for the analysis of samples with sufficiently high fullerene concentration. Since the presence of C_{60} in cosmetic products was previously reported [40,41] at concentration levels up to 1.1 mg kg^{-1}, and in these samples no other fullerenes are applied, two cosmetic products containing this compound were selected to evaluate the applicability of MECC. C_{60} was found at 1.86 ± 0.07 mg L^{-1} (anti-aging serum) and 2.77 ± 0.16 mg kg^{-1} (face mask) concentration levels. The same anti-aging serum sample was analyzed in our previous work by LC-MS [21], reporting C_{60} at a concentration 1.93 ± 0.15 mg L^{-1} confirming the result obtained by MECC. Since no organic solvents are used in MECC, the proposed method is less contaminant than the LC-MS method which requires the use of a high amount of toluene in the mobile phase. Nevertheless, MECC implies two time-

consuming steps, the solubilization of fullerenes in the SDS aqueous solution and the sample preparation.

4.2. Polyhydroxy- and carboxy-fullerene derivatives

In MECC, the buffer composition and concentration showed a significant influence on the electrophoretic pattern of the peaks of polyhydroxy- and carboxy-fullerene derivatives (Figure 4). As expected, the decrease in the EOF produced an increase in the migration times of the compounds which was very significant at high buffer concentrations (~ 50 % increase). For instance, for C_{60}CHCOOH and C_{60}-pyrr tris acid (peak B) an increase from 4.3 min and 4.2 min, respectively at 1 mM sodium tetraborate up to 8.5 min and 10.3 min, respectively at 15 mM sodium tetraborate-15 mM sodium phosphate was observed. Moreover, for concentrations higher than 5 mM sodium tetraborate- 5mM sodium phosphate, highly broad and distorted peaks were obtained. The highly skewed peaks with long tails obtained for the compounds, as the ones observed for C_{60}-pyrr tris acid at 15 mM sodium tetraborate-15mM sodium phosphate for example (Figure 4), prompted the thought that several species with different sizes or charges that migrate with slightly different velocities were present. The observed behavior suggests that large aggregates are formed at high buffer concentration values. As a first step to understand the behavior of these compounds in MECC, the morphology and aggregation degree of the analytes was studied using TEM. As an example, Figure 6 shows the micrographs obtained for C_{60}-pyrr tris acid and $C_{60}(OH)_{24}$ in 100 mM SDS and 10 mM sodium tetraborate-10 mM sodium phosphate. The images show some differences between the aggregate structures and shapes of these compounds and the presence of polidisperse aggregates can be observed in both cases. The carboxy-fullerene derivatives presented large aggregates and spherical and irregular shaped structures of various sizes whereas the polyhydroxy-fullerene derivatives presented mainly polycrystalline structures. As shown, complex branched structures were formed in these conditions which were so strongly aggregated that it was difficult to obtain an average particle size.

The aggregate sizes of the compounds at different buffer composition and concentrations (1 mM sodium tetraborate and sodium tetraborate- sodium phosphate from 2.5 mM to 10 mM of each salt component) and SDS concentrations (from 2 mM to 30 mM) were determined by AF4 with UV detection. The hydrodynamic radii (r_H) of

the particles were calculated from the retention time at the maximum of the peak height using standard AF4 theory [42]. Figure 7A shows an example of the fractograms obtained for C_{60}-pyrr tris acid and $C_{60}(OH)_{24}$ using 2 mM SDS and 1 mM sodium tetraborate as carrier solution. At these conditions, the carboxy-fullerene derivatives eluted in fractions of different aggregation degree and presented at least 2 separated peaks, one corresponding to small particles (≈ 10 nm) and a major peak corresponding to big aggregates with a calculated r_H up to 55 nm. The fractograms obtained for $C_{120}(OH)_{30}$ and $C_{60}(OH)_{24}$ revealed in each case one tailed peak presenting smaller particles sizes than the carboxy-fullerene derivatives, with a r_H calculated at the maximum of the peak height of approx 6 nm and 7 nm, respectively. An increase of the buffer concentration in the carrier solution produced a significant decrease of the peak areas of the carboxy-fullerenes which was caused by an enhanced adsorption of these particles to the AF4 membrane as they settled out of suspension. In contrast, this effect was not observed for the polyhydroxy-fullerene derivatives, due to their higher water solubility and significantly smaller sizes than the carboxy-derivatives. Figure 7B shows, as an example, the fractograms obtained for $C_{60}(OH)_{24}$ using 2 mM SDS and different buffer type and concentrations. As shown, tailing peaks were observed as in the CE experiments probably due to the presence of unresolved higher order aggregates. The change in the elution profile of the polyhydroxy-fullerene derivatives (*i.e.*, retention time shift, broader peaks) at higher buffer concentrations was accompanied by an increase in the calculated r_H at the maximum of the peak height, from approx. 6 nm ($C_{120}OH)_{30}$) and 7 nm ($C_{60}OH)_{24}$) (1 mM sodium tetraborate) up to 13 nm ($C_{120}OH)_{30}$) and 15 nm ($C_{60}OH)_{24}$) (10 mM sodium tetraborate-10 mM sodium phosphate). Therefore, the broad and distorted peaks obtained for the studied compounds by capillary electrophoresis at high buffer concentrations seem to be due to increased aggregation and to the presence of fractions of different aggregation degree.

The AF4 results showed that the presence of SDS micelles does not seem to increase the aggregation of fullerenes but favors the separation of particles of different aggregate sizes. Figure 7B shows the fractograms obtained for $C_{60}(OH)_{24}$ in the presence (30 mM SDS) and absence (2 mM SDS) of micelles. As can be seen, in the presence of micelles, 3 unresolved peaks were obtained, corresponding to particles with different aggregation degree with an average r_H of 4 nm, 6 nm and 10 nm. Similar behavior was observed for the other studied fullerenes indicating that the presence of micelles allows distinguishing between aggregates of different sizes in the samples

probably due to their different partition/complexation with the micelles. This could explain the multiple and broad peaks observed in MECC and the improvement in peak shape with the decrease of SDS concentration (Figure 5).

Over the studied pH range (3-12.5), the studied compounds maintained a substantial charge and were detected in normal polarity. These results are in agreement with previous studies reporting that fullerols present negative surface charge over a wide pH range (pH >3), implying a certain proportion of deprotonated surface sites, even at acidic conditions [37,43]. However, to the best of our knowledge, the pKa values of these compounds are not known accurately. As expected, higher migration times were obtained when decreasing the pH because of a slower EOF (Figure S1). Under acidic conditions, broad and distorted peaks with high migration times were obtained.

5. Conclusions

Complementary information about the aggregation of four surface modified fullerenes in aqueous solutions of different buffer and SDS concentrations was obtained by using three different techniques (CE, AF4 and TEM). The observed significant differences in the electrophoretic peak profiles of the studied compounds revealed that CE techniques are able to capture the changes in their aggregation state. The broad, multiple and distorted peaks obtained in MECC (at high buffer and SDS concentrations) can be related to the increased aggregation that generated particles of different sizes, whereas by working in CZE conditions sharper peaks were obtained. AF4 provided information about the changes in the aggregate sizes of the selected fullerenes at the tested conditions. The calculated particle hydrodynamic radii values showed that high buffer concentration values promote the aggregation of the particles while the presence of micelles allows distinguishing between aggregates of different sizes. As regards the aggregate structures, the obtained TEM images revealed the formation of highly branched and complex aggregates in the evaluated MECC conditions. Therefore, the combination of these techniques offers a wide picture of the aggregation of fullerenes in aqueous solutions.

Acknowledgments

The authors gratefully acknowledge for the financial support received from the Spanish Ministry of Economy and Competitiveness under the project CTQ2012-30836, and from the Agency for Administration of University and Research Grants (Generalitat de Catalunya, Spain) under the project 2014 SGR-539. Alina Astefanei acknowledges the Spanish Ministry of Economy and Competitiveness for a Ph.D. grant (FPI-MICINN) which enabled her to carry out this research at the University of Barcelona and as a visiting scientist at the University of Amsterdam. We also thank Carmen Lopez and Nieves Hernandez (CCiTUB, University of Barcelona) for help with the TEM analysis.

Conflict of interest

The authors declare no conflict of interest.

References

1. Kroto HW, Heath JR, O'Brien SC, Curl RF, Smalley RE (1985) C60: buckminsterfullerene. Nature 318:162-163

2. Tagmatarchis N, Shinohara H (2001) Fullerenes in medicinal chemistry and their biological applications. Mini-Rev Med Chem 1:339-348

3. Xiao L, Takada H, Gana X, Miwa N (2006) The water-soluble fullerene derivative 'Radical Sponge' exerts cytoprotective action against UVA irradiation but not visible-light-catalyzed cytotoxicity in human skin keratinocytes. Bioorg Med Chem Lett 16:1590-1595

4. Kronholm D, Hummelen JC (2007) Fullerene-based n-type semiconductors in organic electronics. Mater Matters (Milwaukee, WI, U S) 2:16-19

5. Meng H, Xing G, Sun B, Zhao F, Lei H, Li W, Song Y, Chen Z, Yuan H, Wang X, Long J, Chen C, Liang X, Zhang N, Chai Z, Zhao Y (2010) Potent angiogenesis inhibition by the particulate form of fullerene derivatives. ACS Nano 4:2773-2783

6. Dugan LL, Lovett EG, Quick KL, Lotharious J, Lin TT, O'Malley KL (2001) Fullerene-based antioxidants and neurodegenerative disorders. Parkinson Relat Disord 7:243-246

7. Bosi S, Da Ros T, Spalluto G, Prato M (2003) Fullerene derivatives: an attractive tool for biological applications. Eur J Med Chem 38:913-923

8. Sitharaman B, Asokan S, Rusakova I, Wong MS, Wilson LJ (2004) Nanoscale Aggregation Properties of Neuroprotective Carboxyfullerene (C3) in Aqueous Solution. Nano Lett 4:1759-1762

9. Friedman SH, DeCamp DL, Sijbesma RP, Srdanov G, Wudl F, Kenyon GL (1993) Inhibition of the HIV-1 protease by fullerene derivatives: model building studies and experimental verification. J Am Chem Soc 115:6506-6509

10. Yamago S, Tokuyama H, Nakamura E, Kituchi K, Kananishi S, Sueki K, Nakahara H, Enmoto S, Ambe F (1995) In vivo biological behavior of a water-miscible fullerene: 14C labeling, absorption, distribution, excretion and acute toxicity. Chem Biol 2:385-389

11. Nel AE, Madler L, Velegol D, Xia T, Hoek EMV, Somasundaran P (2009) Understanding biophysicochemical interactions at the nano-bio interface. Nano Mater 8:543-547

12. Vileno B, Marcoux PR, Lekka M, Sienkiewicz A, Feher T, Forro L (2006) Spectroscopic and Photophysical Properties of a Highly Derivatized C60 Fullerol. Adv Funct Mater 16:120-128

13. Pickering KD, Wiesner MR (2005) Fullerol-sensitized production of reactive oxygen species in aqueous solution. Environ Sci Technol 39:1359-1365

14. Sayes CM, Fortner JD, Guo W, Lyon D, Boyd AM, Ausman KD, Tao YJ, Sitharaman B, Wilson LJ, Hughes JB, West JL, Colvin VL (2004) The Differential Cytotoxicity of Water-Soluble Fullerenes. Nano Lett 4:1881-1887

15. Astefanei A, Núñez O, Galceran MT (2015) Characterisation and analysis of fullerenes: A critical review. Anal Chim Acta doi:10.1016/j.aca.2015.03.025:

16. Handy RD, Owen R, Valsami-Jones E (2008) The ecotoxicology of nanoparticles and nanomaterials: current status, knowledge gaps, challenges, and future needs. Ecotoxicology 17:315-325

17. Klaine SJ, Alvarez PJJ, Batley GE, Fernandes TF, Handy RD, Lyon DY, Mahendra S, McLaughlin MJ, Lead JR (2008) Nanomaterials in the environment: behavior, fate, bioavailability, and effects. Environ Toxicol Chem 27:1825-1851

18. A. Astefanei, O. Núñez, M.T. Galceran, Liquid Chromatography in the Analysis of Fullerenes, in: S.B. Ellis (Ed.), Fullerenes, Chemistry, Natural Sources and Technological Applications, Nova Science Publishers, New York, 2014, pp. 35-63.

19. Chao TC, Song G, Hansmeier N, Westerhoff P, Herckes P, Halden RU (2011) Characterization and Liquid Chromatography-MS/MS Based Quantification of Hydroxylated Fullerenes. Anal Chem 83:1777-1783

20. Silion M, Dascalu A, Pinteala M, Simionescu BC, Ungurenasu C (2013) A study on electrospray mass spectrometry of fullerenol C60(OH)24. Beilstein J Org Chem 9:1285-1295

21. Astefanei A, Núñez O, Galceran MT (2012) Non-aqueous capillary electrophoresis separation of fullerenes and C60 fullerene derivatives. Anal Bioanal Chem 404:307-313

22. Wan TSM, Leung GNW, Tso TSC, Komatsu K, Murata Y (1995) Non-aqueous capillary electrophoresis as a new method for the separation of fullerenes. Proc - Electrochem Soc 95:1474-1487

23. Su HL, Kao WC, Lee Cy, Chuang SC, Hsieh YZ (2010) Separation of open-cage fullerenes using nonaqueous capillary electrophoresis. J Chromatogr A 1217:4471-4475

24. Treubig JM, Brown PR (2000) Novel approach to the analysis and use of fullerenes in capillary electrophoresis. J Chromatogr , A 873:257-267

25. Cerar J, Pompe M, Gucek M, Cerkovnik J, Skerjanc J (2007) Analysis of sample of highly water-soluble Th-symmetric fullerenehexamalonic acid C66(COOH)12 by ion-chromatography and capillary electrophoresis. J Chromatogr A 1169:86-94

26. Tamisier-Karolak SL, Pagliarusco S, Herrenknecht C, Brettreich M, Hirsch A, Ceolin R, Bensasson RV, Szwarc H, Moussa F (2001) Electrophoretic behavior of a highly water-soluble dendro[60]fullerene. Electrophoresis 22:4341-4346

27. Chan KC, Patri AK, Veenstra TD, McNeil SE, Issaq HJ (2007) Analysis of fullerene-based nanomaterial in serum matrix by CE. Electrophoresis 28:1518-1524

28. Bermudez O, Forciniti D (2004) Aggregation and denaturation of antibodies: a capillary electrophoresis, dynamic light scattering, and aqueous two-phase partitioning study. J Chromatogr B :

29. Sabella S, Quaglia M, Lanni C, Racchi M, Govoni S, Caccacialanza G, Calligaro A, Belloti V, De Lorenzi E (2004) Capillary electrophoresis studies on the aggregation process of -amyloid 1-42 and 1-40 peptides. Electrophoresis 25:3186-3194

30. Pryor E, Kotarek JA, Moss M, Hestekin CN (2011) Monitoring Insulin Aggregation via Capillary Electrophoresis. Int J Mol Sci 12:9369-9388

31. Wahlund KG, Giddings JC (1987) Properties of an asymmetrical flow field-flow fractionation channel having one permeable wall. Anal Chem 59:1332-1339

32. Schimph, M.E., Caldwell, K. and Giddings, J.C (2000), Field flow-field fractionation handbook, John Wiley & Sons, Inc., New York.

33. Baalousha M, Stolpe B, Lead JR (2011) Flow field-flow fractionation for the analysis and characterization of natural colloids and manufactured nanoparticles in environmental systems: a critical review. J Chromatogr A 1218:4078-4103

34. Isaacson CW, Bouchard D (2010) Asymmetric flow field flow fractionation of aqueous C60 nanoparticles with size determination by dynamic light scattering and quantification by liquid chromatography atmospheric pressure photo-ionization mass spectrometry. J Chromatogr A 1217:1506-1512

35. Herrero P, Bäuerlein PS, Emke E, Pocurull E, de Voogt P (2014) Asymmetrical flow field-flow fractionation hyphenated to Orbitrap high resolution mass spectrometry for the determination of (functionalised) aqueous fullerene aggregates. J Chromatogr A 1356:277-282

36. Kato H, Shinohara N, Nakamura A, Horie M, Fujita K, Takahashi K, Iwahashi H, Endoh S, Kinugasa S (2010) Characterization of fullerene colloidal suspension in a cell culture medium for in vitro toxicity assessment. Mol BioSyst 6:1238-1246

37. Assemi S, Tadjiki S, Donose BC, Nguyen AV, Miller JD (2010) Aggregation of Fullerol C60(OH)24 Nanoparticles as Revealed Using Flow Field-Flow Fractionation and Atomic Force Microscopy. Langmuir 26:16063-16070

38. Bensasson RV, Bienvenue E, Dellinger M, Leach S, Seta P (1994) C60 in Model Biological Systems. A Visible-UV Absorption Study of Solvent-Dependent Parameters and Solute Aggregation. J Phys Chem 98:3492-3500

39. Torres VM, Posa M, Srdjenovic B, Simplicio AL (2011) Solubilization of fullerene C60 in micellar solutions of different solubilizers. Colloids Surf , B 82:46-53

40. Chae SR, Hotze EM, Xiao Y, Rose J, Wiesner MR (2010) Comparison of methods for fullerene detection and measurements of reactive oxygen production in cosmetic products. Environ Eng Sci 27:797-804

41. Benn TM, Westerhoff P, Herckes P (2011) Detection of fullerenes (C60 and C70) in commercial cosmetics. Environ Pollut 159:1334-1342

42. Schimph, M.E., Caldwell, K. and Giddings, J.C (2000), Field flow-field fractionation handbook, John Wiley & Sons, Inc., New York.

43. Brant JA, Labille J, Robichaud CO, Wiesner M (2007) Fullerol cluster formation in aqueous solutions: Implications for environmental release. J Colloid Interface Sci 314:281-288

Figure captions:

Figure 1. Structures and abbreviations of the studied fullerenes.

Figure 2. MECC electropherograms of (A) SDS[C_{60}] (25 mg L^{-1}), (B) facial mask product (a), the same product fortified with 3 mg L^{-1} of C_{60} (b); BGE: 100 mM SDS, 10 mM sodium tetraborate-10 mM sodium phosphate (pH=9.4); voltage: + 20 kV.

Figure 3. MECC electropherograms of: 1: $C_{60}(OH)_{24}$ (25 mg L^{-1}); 2: $C_{120}(OH)_{30}$ (25 mg L^{-1}); 3: C_{60}-pyrr tris acid (25 mg L^{-1}); 4: $C_{60}CHCOOH$ (25 mg L^{-1}); BGE: 100 mM SDS, 10 mM sodium tetraborate-10 mM sodium phosphate (pH=9.4); voltage: + 20 kV; λ= 254 nm.

Figure 4. MECC electropherograms of the studied fullerenes at different buffer concentrations: (a) 15 mM sodium tetraborate-15 mM sodium phosphate; (b) 10 mM sodium tetraborate-10 mM sodium phosphate; (c) 2.5 mM sodium tetraborate-2.5 mM sodium phosphate and (d) 1 mM sodium tetraborate; other BGE conditions: 100 mM SDS; voltage: + 20 kV.

Figure 5. Electropherograms of the selected fullerenes at different SDS concentrations: (a) 100 mM SDS; (b) 40 mM SDS; (c) 2 mM SDS; other BGE conditions: 1 mM sodium tetraborate; voltage: + 20 kV.

Figure 6: TEM pictures of C_{60}-pyrr tris acid and $C_{60}(OH)_{24}$ aggregates.

Figure 7. (A) Fractograms of $C_{60}(OH)_{24}$ and C_{60}-pyrr tris acid; carrier solution: 2 mM SDS and 1mM sodium tetraborate, pH=9.2 and (B) Fractograms of $C_{60}(OH)_{24}$; carrier solution: (a) 30 mM SDS and 1 mM sodium tetraborate, (b) 2 mM SDS and 10 mM sodium tetraborate-10 mM sodium phosphate, and (c) 2 mM SDS and 1 mM sodium tetraborate. TDE flow programming with a delay/decay time of 3 min (C_{60}-pyrr tris acid) and 7 min $C_{60}(OH)_{24}$. For the experimental conditions used see text.

Figure S1. pH effect (3-12.5) on the migration times as observed by CZE of 1: $C_{60}(OH)_{24}$; 2: $C_{120}(OH)_{30}$; 3: C_{60}-pyrr tris acid; 4: $C_{60}CHCOOH$; BGE: 2 mM SDS in 1 mM sodium tetraborate; voltage: + 20 kV; λ= 254 nm.

Table 1. Instrumental quality parameters

	LODs (mg L^{-1})	LOQs (mg L^{-1})	run-to-run precision (% RSD; n=5)			day-to-day precision (% RSD; n=5 x 3)		
			t_m (min)	Concentration (low level)[a]	Concentration (medium level)[b]	t_m (min)	Concentration (low level)[a]	Concentration (medium level)[b]
C_{60}	0.8	2.4	0.2	5.1	2.4	1.2	6.5	2.1
C_{70}	2.2	6.6	0.4	7.8	4.6	1.3	14.3	9.2
C_{60}-pyrr	0.6	1.8	0.3	4.3	2.3	1.0	5.7	2.0

[a] LOQ

[b] 10 mg L^{-1} (C_{60} and C_{60} pyrr) and 5 mg L^{-1} (C_{70})

Figure 1

C_{60}

C_{70}

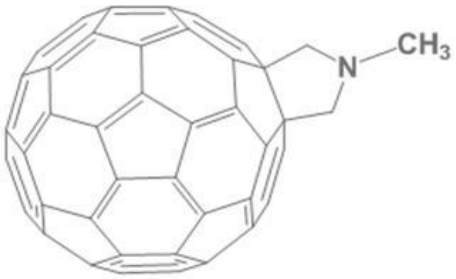

C_{60}-pyrr

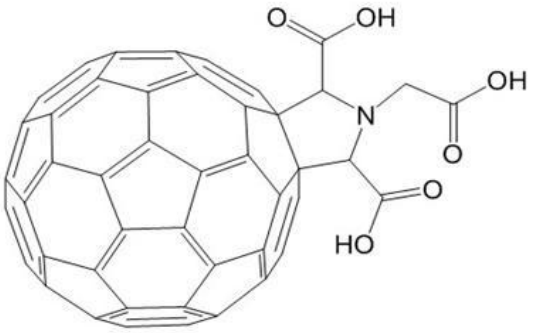

C_{60}-pyrr tris acid

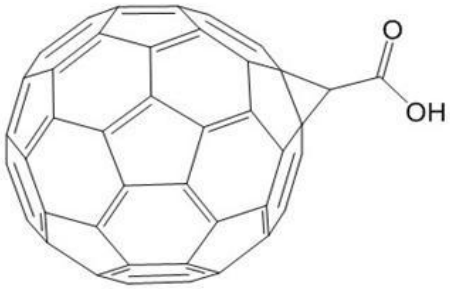

$C_{60}CHCOOH$

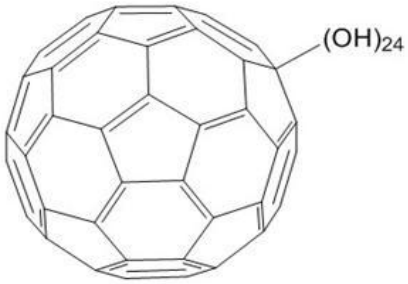

$C_{60}(OH)_{24}$

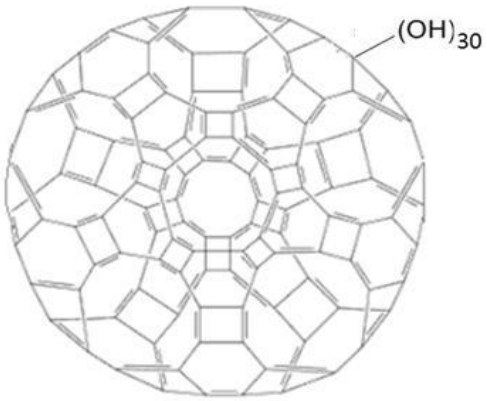

$C_{120}(OH)_{30}$

Figure 2

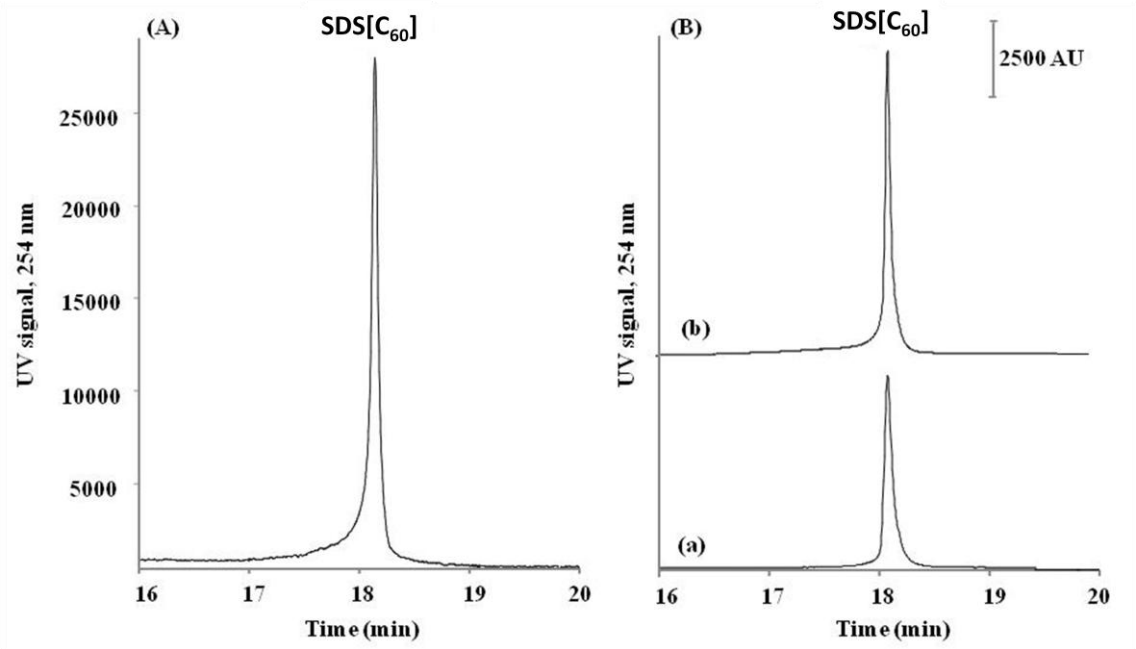
(A)
SDS[C60]
25000
20000
15000
10000
5000
UV signal, 254 nm
16
17
18
19
20
Time (min)
(B)
SDS[C60]
2500 AU
(b)
(a)
UV signal, 254 nm
16
17
18
19
20
Time (min)

Figure 3

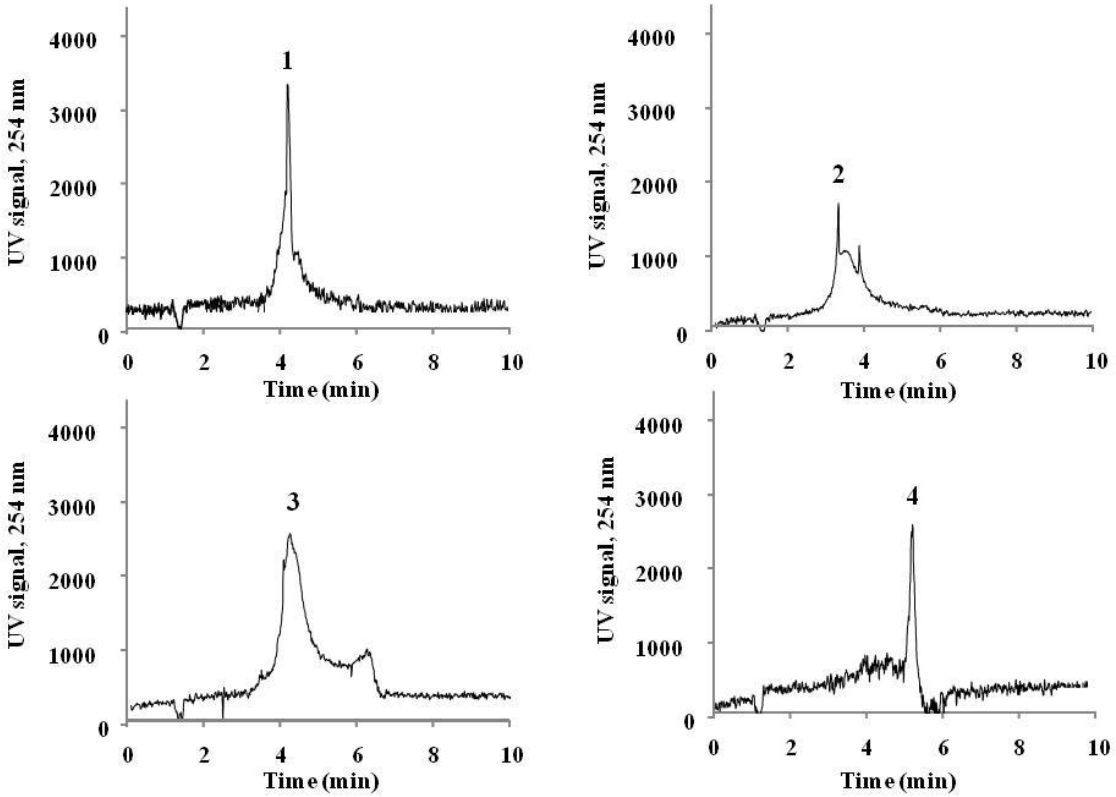

Figure 4

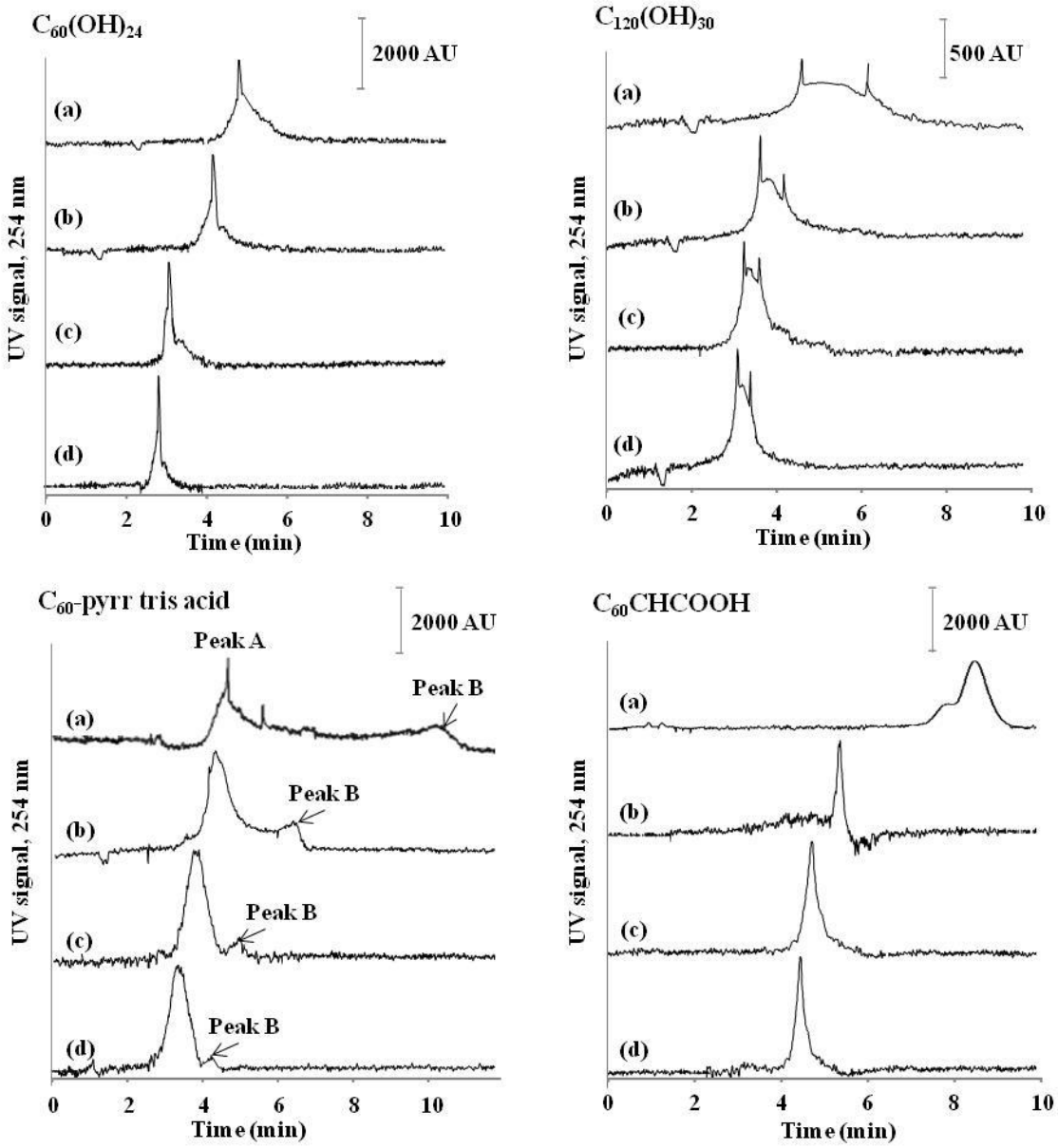
C60(OH)24
2000 AU
(a)
(b)
(c)
(d)
UV signal, 254 nm
0
2
4
6
8
10
Time (min)
C120(OH)30
500 AU
(a)
(b)
(c)
(d)
UV signal, 254 nm
0
2
4
6
8
10
Time (min)
C60-pyrr tris acid
2000 AU
Peak A
Peak B
Peak B
Peak B
Peak B
(a)
(b)
(c)
(d)
UV signal, 254 nm
0
2
4
6
8
10
Time (min)
C60CHCOOH
2000 AU
(a)
(b)
(c)
(d)
UV signal, 254 nm
0
2
4
6
8
10
Time (min)

Figure 5

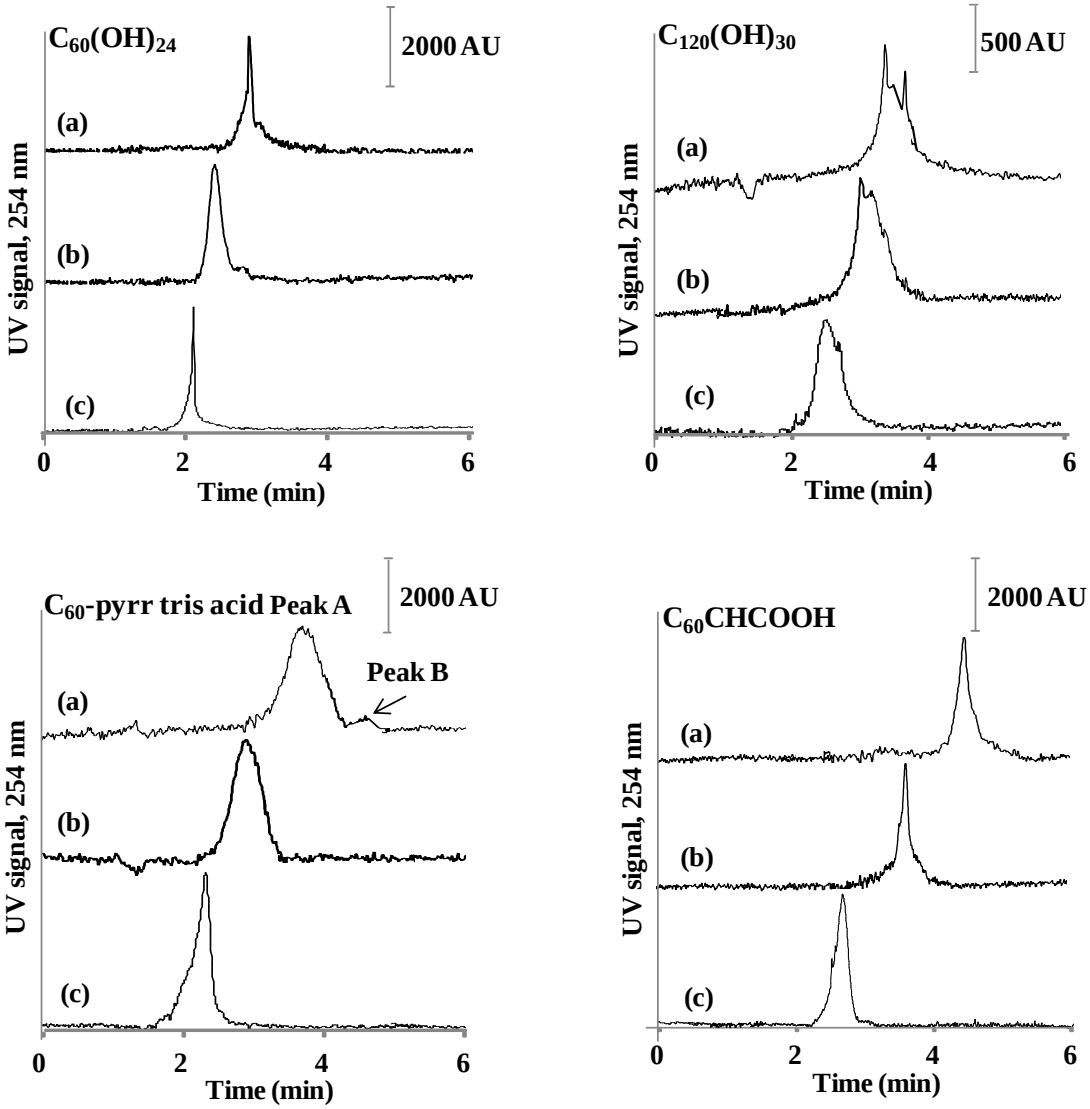
C60(OH)24
2000 AU
(a)
(b)
(c)
UV signal, 254 nm
0
2
4
6
Time (min)
C120(OH)30
500 AU
(a)
(b)
(c)
UV signal, 254 nm
0
2
4
6
Time (min)
C60-pyrr tris acid Peak A
2000 AU
Peak B
(a)
(b)
(c)
UV signal, 254 nm
0
2
4
6
Time (min)
C60CHCOOH
2000 AU
(a)
(b)
(c)
UV signal, 254 nm
0
2
4
6
Time (min)

Figure 6

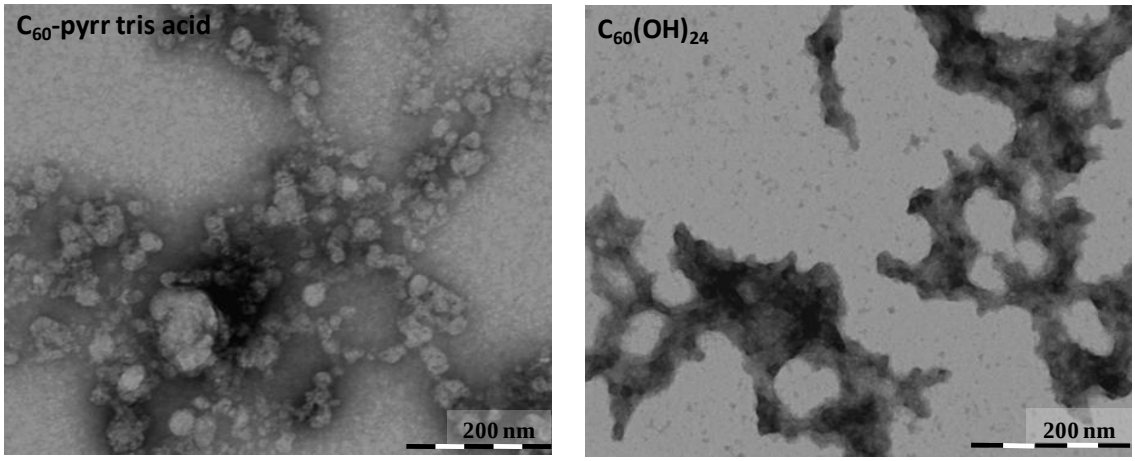

Figure 7

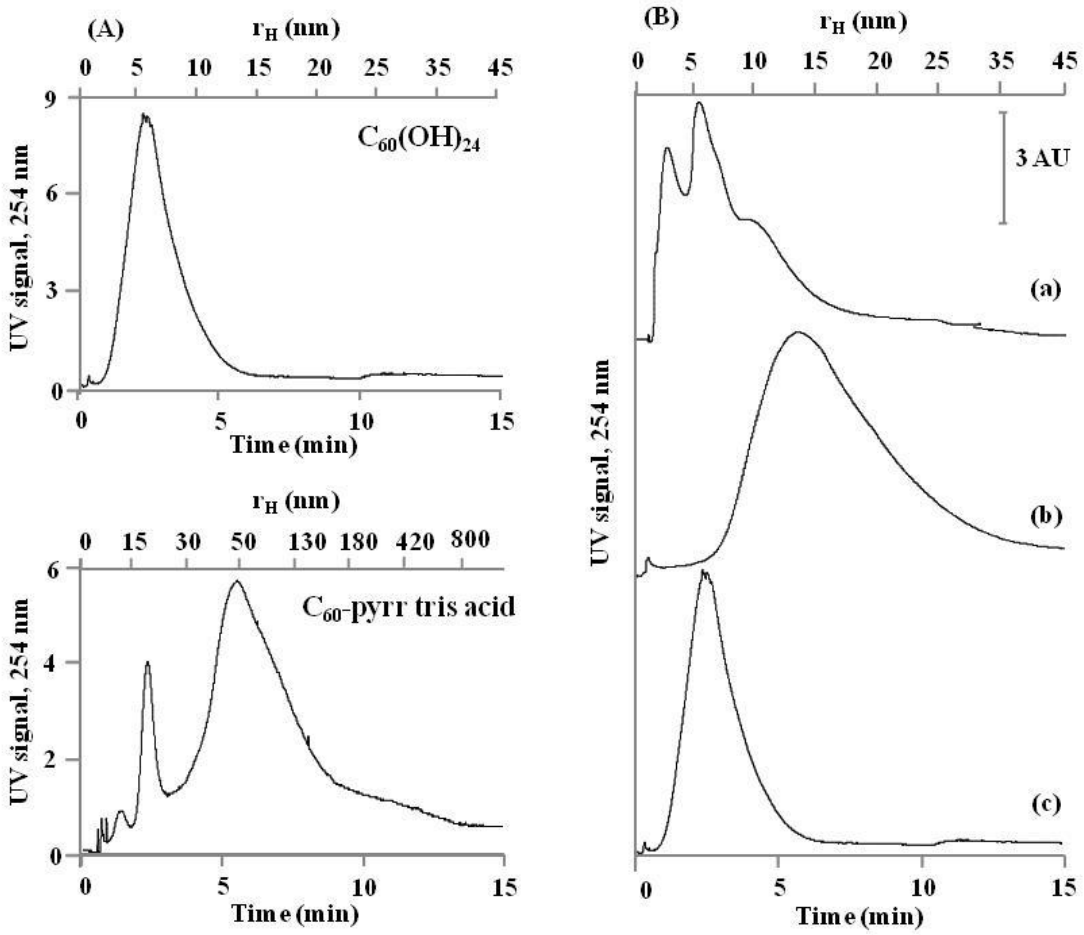
(A)
r_H (nm)
0 5 10 15 20 25 35 45
$C_{60}(OH)_{24}$
UV signal, 254 nm
Time (min)
r_H (nm)
0 15 30 50 130 180 420 800
C_{60}-pyrr tris acid
UV signal, 254 nm
Time (min)
(B)
r_H (nm)
0 5 10 15 20 25 35 45
3 AU
(a)
(b)
(c)
UV signal, 254 nm
Time (min)